Sunscreens with the New MCE Filter Cover the Whole UV Spectrum: Improved UVA1 Photoprotection In Vitro and in a Randomized Controlled Trial

Claire Marionnet[1], Romain de Dormael[1], Xavier Marat[1], Angélina Roudot[2], Julie Gizard[1], Emilie Planel[1], Carine Tornier[3], Christelle Golebiewski[1], Philippe Bastien[1], Didier Candau[2] and Françoise Bernerd[1]

Background: UVA1 rays (340–400 nm) contribute to carcinogenesis, immunosuppression, hyperpigmentation, and aging. Current sunscreen formulas lack sufficient absorption in the 370–400 nm wavelengths range. Recently, a new UVA1 filter, Methoxypropylamino Cyclohexenylidene Ethoxyethylcyanoacetate (MCE) exhibiting a peak of absorption at 385 nm, was approved by the Scientific Committee on Consumer Safety for use in sunscreen products. These studies evaluated, in a three-dimensional skin model and in vivo, the protection afforded by state-of-the-art sunscreen formulations enriched with MCE. **Trial design:** This study is a monocentric, double-blinded, randomized, and comparative trial. This study is registered at ClinicalTrials.gov with the identification number NCT04865094. **Methods:** The efficacy of sunscreens with MCE was compared with that of reference formulas. In a three-dimensional skin model, histology, protein, and gene expression were analyzed. In the clinical trial, pigmentation was analyzed in 19 volunteers using colorimetric measurements and visual scoring. **Results:** MCE addition in reference formulas enlarged the profile of absorption up to 400 nm; reduced UVA1-induced dermal and epidermal alterations at cellular, biochemical, and molecular levels; and decreased UVA1-induced pigmentation. **Conclusions:** Addition of MCE absorber in sunscreen formulations leads to full coverage of UV spectrum and improved UVA1 photoprotection. The data support benefits in the long term on sun-induced consequences, especially those related to public health care issues.

JID Innovations (2022);**2:**100070 doi:10.1016/j.xjidi.2021.100070

INTRODUCTION

Exposure to solar UVR is the major environmental aggressor for the skin, responsible for skin cancer. Squamous cell carcinoma has been associated with chronic cumulative exposure all life long, basal cell carcinoma has been associated with both chronic and intermittent intense UV exposure, especially early in life (Milon et al., 2014; Verkouteren et al., 2017), whereas melanoma is associated with intermittent recreational exposure or sunburn history during childhood (Dennis et al., 2008; Gandini et al., 2011). Besides skin cancers, acute or repeated sun exposure contributes to numerous harmful effects such as photoimmunosuppression, viral reactivation, premature skin aging, and pigmentary disorders (Gibbs and Norval, 2013; Ortonne, 1990; Rittié and Fisher, 2015).

Solar UV reaching the earth includes UVB (290–320 nm), UVA2 (320–340 nm), and UVA1 rays (340–400 nm). UVB rays represent 5% maximum of solar UV but induce potentially mutagenic DNA photoproducts and are responsible for erythema, skin pigmentation, photoimmunosuppression, and skin cancers. In turn, UVA1 rays account for >80% of solar UV received on the earth. Less energetic than UVB rays but with higher penetration properties, they can reach the deep dermis. In the last decade, their contribution in photoaging (Wang et al., 2014), photoimmunosuppression (Damian et al., 2011; Matthews et al., 2010), polymorphic light eruptions (Badri and Schlessinger, 2020; Lembo and Raimondo, 2018), herpes simplex virus reactivation (Kerr et al., 2012; York and Jacobe, 2010), photocarcinogenesis (de Laat et al., 1997; Ley and Fourtanier, 2000), and hyperpigmentation (Marionnet et al., 2017; Ravnbak and Wulf, 2007) was pointed out. At the biological level, they lead to ROS generation, induce DNA lesions and mutagenesis in epidermal basal cells, damage skin dermis, and alter the expression of genes involved in a large panel of essential functions and pathways, including cancer, proliferation, apoptosis, development, innate immunity, extracellular matrix, response to stress/oxidative stress, and metabolism

[1]*L'Oréal Research and Innovation, Aulnay-sous-Bois, France;* [2]*L'Oréal Research and Innovation, Chevilly-Larue, France; and* [3]*Episkin, Lyon, France*

Correspondence: Claire Marionnet, L'Oréal Research and Innovation, 1 Avenue Eugène Schueller, 93600 Aulnay-sous-Bois, France. E-mail: claire.marionnet@rd.loreal.com

Abbreviations: FC, fold change; ITA°, individual typology angle; KC, keratinocyte; MCE, Methoxypropylamino Cyclohexenylidene Ethoxyethylcyanoacetate; MMP, matrix metalloproteinase; SPF, sun-protection factor

Received 17 May 2021; revised 27 October 2021; accepted 28 October 2021; accepted manuscript published online XXX; corrected proof published online XXX

Cite this article as: JID Innovations 2022;2:100070

(Marionnet et al., 2014; Rünger et al., 2012; Tewari et al., 2013).

To limit harmful skin damage due to sun exposure, World Health Organization, United States Environmental Protection Agency, and dermatological academies recommend photoprotective behaviors, including the use of sunscreen with effective UVB and UVA absorption (https://www.who.int/uv/sun_protection/en/; https://www.epa.gov/sunsafety/action-steps-sun-safety; https://www.aad.org/public/everyday-care/sun-protection/sunscreen/how-to-select-sunscreen, respectively). To this end, sunscreen products are composed of UV absorbers whose combination determines the overall absorption profile of the final formula (Daly et al., 2016; Moyal, 2012). Today's state-of-the-art sunscreens can efficiently filter UVB, UVA2, and UVA1 up to ~370 nm. However, they lack a 370–400 nm sufficient absorption in the UVA1 domain owing to the absence of efficient authorized UV filters in this wavelengths range. To show the benefit of providing the appropriate photoprotection in this UVA1 wavelength range, a proof-of-concept study has been performed using laboratory tools UVA1-absorbing molecules in prototype formulations (Marionnet et al., 2018). On the basis of these mandatory positive efficacy results, the whole process of developing a new UVA1 filter was engaged, taking into account the regulatory (human and environmental safety) and industrial feasibility constraints for molecule selection.

Therefore, to our knowledge, a previously unreported cyclic merocyanine UVA1 absorber, Methoxypropylamino Cyclohexenylidene Ethoxyethylcyanoacetate (MCE), was synthesized and enabled coverage of the 360–400 nm wavelengths range (Winkler et al., 2014). MCE dossier was approved by the Scientific Committee on Consumer Safety at the European Commission on the basis of safety and environmental profile and is now listed in the Annex VI of European Union–authorized UV filters. MCE can be used in sunscreen formulations up to 3% (https://ec.europa.eu/health/sites/health/files/scientific_committees/consumer_safety/docs/sccs_o_227.pdf).

This study aimed at investigating the benefit of the MCE filter addition in state-of-the-art sunscreen formulations in UVA1 photoprotection, at the absorption profile level, at the biological level using a three-dimensional human skin model, and in vivo using pigmentation (Persistent Pigment Darkening) as a clinical endpoint.

RESULTS

The MCE filter

The MCE filter exhibited a peak of absorption at 385 nm with an absorption coefficient of 63,052 (investigated in ethanol at 0.02 mM) (Figure 1). The MCE filter showed 100% intrinsic stability in simplex medium, that is, hydroethanolic solution, and stability robustness with regard to different stress, including heat (99% after 2 hours at 90 °C), acid (96–99% after 0.1 M hydrogen chloride at room temperature or 60 °C), and oxidant (98–99% after hydrogen peroxide treatment). MCE also showed 98–99% photostability under exposure to solar simulation even in the presence of more oxygen (Tables 1–3).

The MCE filter was added in state-of-the-art formulations to produce formulations with enlarged absorption in the UVA1

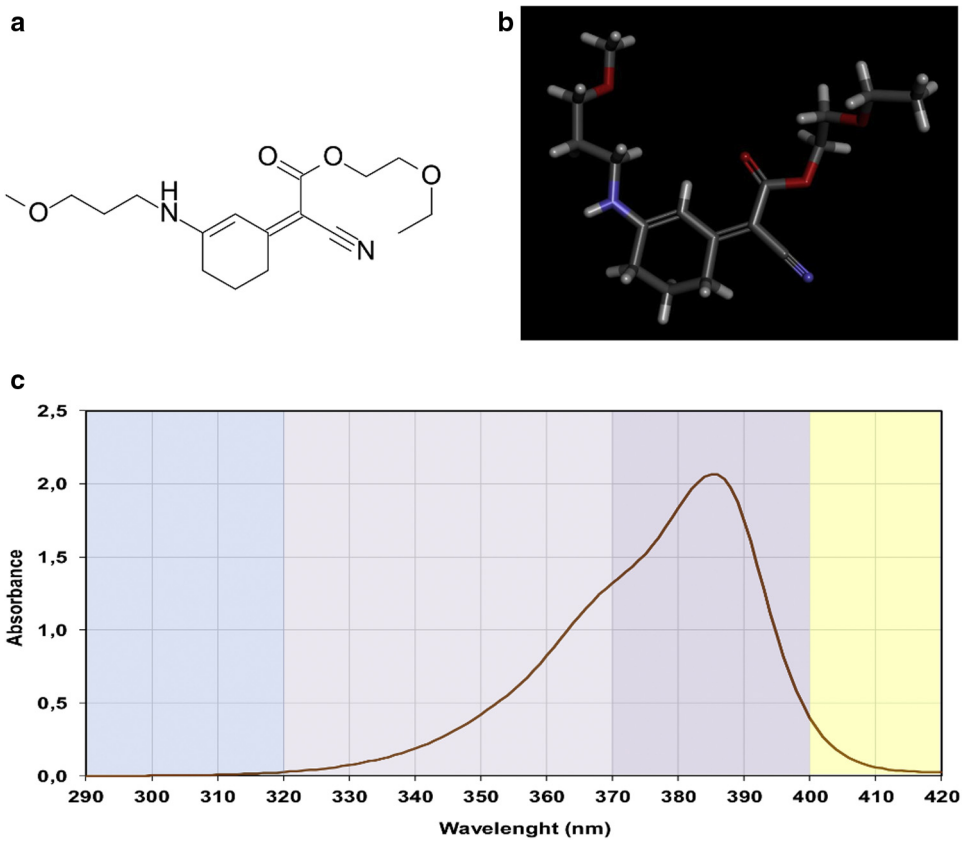

Figure 1. Characteristics of the MCE filter. (**a, b**) Structural and (**c**) absorption characteristics. MCE has a 322.41 g/mol molecular weight. (**a**) Molecular structure of the MCE filter in 2D with a Z configuration. (**b**) Molecular geometry in 3D of the MCE filter issued from the crystal structure (CCDC references JOKPOQ 973065) and visualized with Accelerys Discovery Studio 4.1. (**c**) Absorption spectrum of the MCE filter measured using a spectrophotometer by a 1-cm path length cuvette at 10 mg/l solution or by a 1-mm cuvette at 100 mg/l (measured absorbance every 5 nm). 2D, two-dimensional; 3D, three-dimensional; CCDC, Cambridge Crystallographic Data Center; MCE, Methoxypropylamino Cyclohexenylidene Ethoxyethylcyanoacetate.

Table 1. Intrinsic Stability Performed in a Hydroethanolic Solution

Temperature	Time	% Remaining	Aspect
4 °C	1 month	100	Pale yellow limpid solution
45 °C	1 month	100	Pale yellow limpid solution
4 °C	2 months	100	Pale yellow limpid solution
45 °C	2 months	100	Pale yellow limpid solution

Abbreviations: MCE, Methoxypropylamino Cyclohexenylidene Ethoxyethylcyanoacetate; t, time.

MCE was solubilized in 0.5 g/100 ml water/ethanol 50/50 (v/v) and placed (triplicates) into a controlled temperature oven or fridge. Aliquoting and analytical follow-up were performed on a UPLC/DAD Acquity apparatus (Waters, Milford, MA) after 1 month and 2 months. The chemical stability assay showed that MCE is stable to mild hydrolysis from t 0 up to 2 months even at 45 °C. These results indicate that MCE could be further integrated into cosmetic galenic support containing water.

wavelengths domain. The photoprotection efficiency of the formulations was assessed in vitro and in vivo. The state-of-the-art formulations correspond to formulations having the best profile of filtration (for a determined sun-protection factor [SPF] value) that can be obtained using currently available sunscreen filters, that is, a profile of absorption covering UVB and UVA up to 360–370 nm with a well-balanced UVB–UVA profile.

In vitro study

A three-dimensional human skin model was used to compare the efficacy of three formulas: a state-of-the-art formula (Reference vitro), absorbing UVB and UVA up to 370 nm, and Formulas vitro 0.7% MCE and 1.5% MCE containing the indicated percentage of MCE filter, respectively, enabling UVA1 absorption up to 385 nm and 400 nm, respectively (Figure 2a and b).

Cell and tissue change analysis. The formulations were applied topically onto reconstructed skin and sham exposed or exposed to a single UVA1 dose (40, 60, or 80 J/cm^2). Skins were histologically analyzed, and fibroblasts were immunostained 48 hours later. As previously described, the biologically efficient dose of 40 J/cm^2 UVA1 induced epidermal alterations in upper layers and disappearance of fibroblasts mostly in the upper dermis (Marionnet et al., 2014). At that dose, the Reference vitro exhibited an incomplete photoprotection, with remaining epidermal alterations (Figure 3a) and partial protection of fibroblasts (Figure 3b and c). This lack of protection was emphasized in a UVA1 dose–effect manner. Formulas vitro 0.7% MCE and 1.5% MCE offered better protection than Reference vitro. At 60 J/cm^2, they were able to totally protect from fibroblasts disappearance (Figure 3), with better protection of the epidermal layers, which was complete with Formula vitro 1.5% MCE (Figure 3a). At the highest dose (80 J/cm^2), only Formula vitro 1.5% MCE efficiently protected dermal fibroblasts (Figure 3c). At that dose, the number of fibroblasts was not significantly different between Formula vitro 0.7% MCE and Reference vitro.

Protein expression analysis. UVA1 exposure of reconstructed skins was shown to increase the release of proinflammatory cytokines and matrix metalloproteinases (MMPs) (Marionnet et al., 2014). These markers were used to test the protection of the three formulas after 40, 60, or 80 J/cm^2 of UVA1 exposure (Table 4). Fourty Joules per square centimeter UVA1 significantly increased the levels of MMP1 and proinflammatory proteins IL-1RA, IL-6, and GM-CSF, taking into account dermal cell mortality. IL-8 amount was also 2.7-fold increased, although this was not statistically different from that of the control. At that UVA1 dose, Reference vitro, compared with unprotected condition, decreased the amounts of secreted MMP1, IL-6, and IL-8, reducing them to control values, and, to a lesser extent, GM-CSF. Reference vitro exhibited good protection against the production of the latter proteins, Formulas vitro 0.7% MCE and 1.5% MCE showed no significant difference from the Reference vitro. At that UVA1 dose, IL-1RA secretion was poorly protected by the Reference vitro, whereas Formula vitro 1.5% MCE exhibited significantly better protection than the Reference vitro. Significant differences could be evidenced at 60 and 80 J/cm^2 UVA1 between formulas containing MCE filter and the Reference vitro. At 60 J/cm^2, Formula vitro 0.7% MCE was able to significantly reduce the amounts of MMP1, IL-1RA, IL-6, and GM-CSF ($P < 0.05$). At 80 J/cm^2, this formula still significantly reduced MMP1, IL-6, and also IL-8 amounts, whereas Formula vitro 1.5% MCE enabled the significant decrease of all the tested proteins, compared with the Reference vitro ($P < 0.05$).

Gene expression analysis. In reconstructed skin, UVA1 exposure induced the modulation of expression levels of

Table 2. Acidic and Oxidizing Stability Performed in a Ternary Mixture

Stress Factor	Concentration	Time	Temperature	Remaining (%)	Loss (%)
Acid 0.1 M HCl	0.5%	0 h	Room temperature	99	1
		1 h	Room temperature	98	2
		1 h	60 °C	96	4
Oxidant 5 V H_2O_2	0.6%	0 h	Room temperature	99	1
		2 h	Room temperature	98	2
Temperature	0.5%	2 h	90°C	99	1

Abbreviations: H_2O_2, hydrogen peroxide; HCl, hydrogen chloride; MCE, Methoxypropylamino Cyclohexenylidene Ethoxyethylcyanoacetate.

MCE was solubilized in a 0.5 g/100 ml ternary water/ethanol/isopropanol mixture with the final concentration of 50/40/10 (v/v/v). Duplicates were put in contact with an acidic or oxidizing solution at controlled temperature and time. Aliquoting and analytical follow-up were performed on a UPLC/DAD Acquity apparatus (Waters, Milford, MA). The results showed that MCE is stable to mild acidic hydrolysis and to H_2O_2 oxidizer. This means that MCE could be further integrated into cosmetic galenic support containing water, with adjusted pH lower than neutrality and without any issue regarding the presence of oxygen or oxidizing agent.

Table 3. Intrinsic Photostability Performed in Hydroethanolic Solution

Vial Type	Concentration	Time	Aerobic Contact	Remaining (%)	Loss (%)
Glass vial irradiation	0.5%	24 h	Limited aerobic contact	98	2
			Full aerobic contact	98	2
Quartz cuvette irradiation	0.5%	24 h	Limited aerobic contact	99	1
			Full aerobic contact	98	2

Abbreviations: IR, infrared; MCE, Methoxypropylamino Cyclohexenylidene Ethoxyethylcyanoacetate.

MCE was solubilized in 0.5 g/100 ml water/ethanol 50/50 (v/v), and the different vials were placed in an open glass plate ready for the irradiation step. Solar simulation was performed using a Suntest CPS apparatus (Atlas Material Testing Technology, Mount Prospect, IL) with a xenon arc lamp equipped with a filter cutting <295 nm and in accordance with solar spectral distribution excepting IR (in order not to overheat samples). Duration of the test was 24 hours at room temperature. Vials containing MCE were full (limited aerobic contact) or half (full aerobic contact) filled. Aliquoting and analytical follow-up were performed using a UPLC/DAD Acquity apparatus (Waters, Milford, MA). MCE was intrinsically photostable after exposure to solar simulation. Indeed, MCE did not lose its ability to filter light, especially solar light, and UVA wavelengths over time when exposed to solar simulation in solution. This ability was not compromised in the presence of more oxygen.

numerous transcripts involved in diverse biological pathways (Marionnet et al., 2014). Taking advantage of this molecular information, the photoprotection of the Reference vitro and Formula vitro 1.5% MCE was compared at 40 J/cm^2 UVA1 dose using transcripts level modulations.

To have an overall view of the gene expression modulation induced by UVA1 in reconstructed skins protected or not by formulas, the expression of 27 and 24 transcripts selected on the basis of our previous data and representative of the diversity of biological functions altered after UVA1 exposure (Marionnet et al., 2014) was analyzed in fibroblasts and in keratinocytes (KCs), respectively (Figure 4).

In fibroblasts of reconstructed skins without any formula, the 27 tested genes had their expression modulated by UVA1. The modulation ratio was high ($R > 10$ or $R < 0.1$) for 8 genes, moderate ($5 < R < 10$ or $0.2 < R < 0.1$) for 11genes, and low ($2 < R < 5$ or $0.5 < R < 0.2$) for 8 genes. Pre-application of the Reference vitro formula reduced the number of UVA1-modulated genes with 22 out of 27 genes. In addition, in the Reference vitro–treated samples, the intensities of these modulations were reduced compared with those in the nonprotected samples, with only 4, 4, and 14 genes exhibiting high, moderate, and low levels of modulation, respectively. When the Formula vitro 1.5% MCE was applied, only 11 out of 27 (41%) genes were found modulated after UVA1. Moreover, the intensities of modulation were decreased compared with those for the Reference vitro–treated samples, with three, two, and six genes exhibiting high, moderate, and low modulation levels, respectively (Figure 4a). In KCs, the same pattern of gene expression

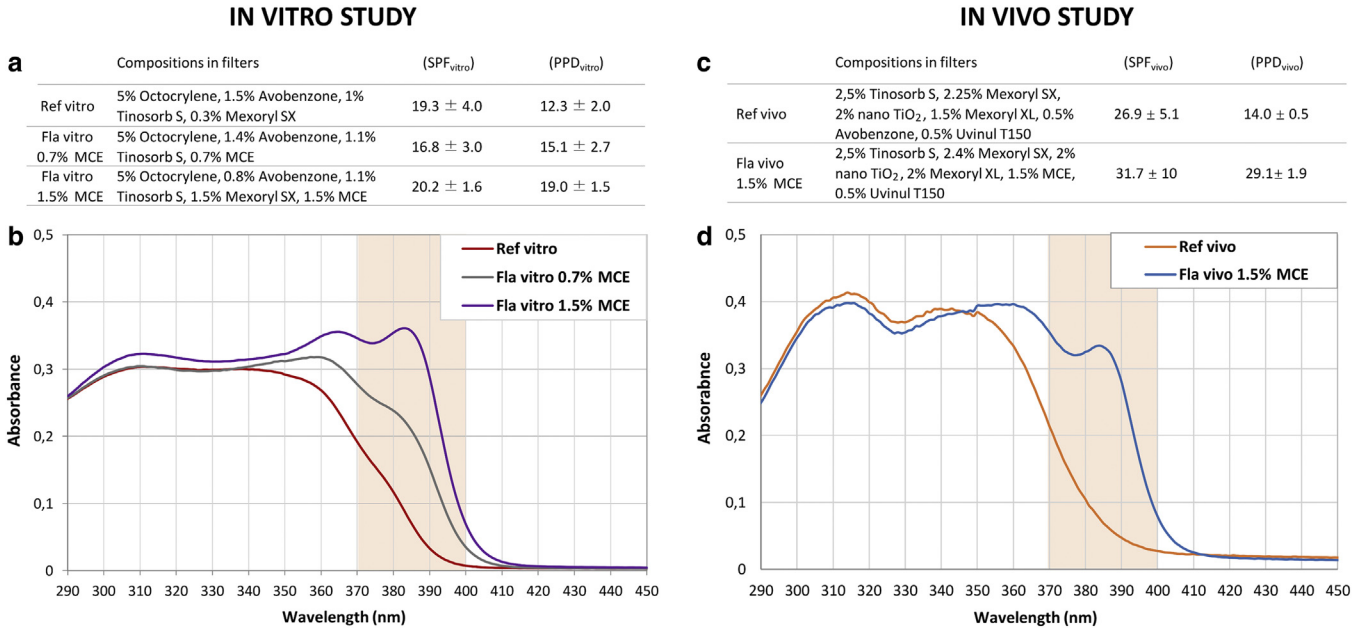

Figure 2. Composition, protection factors and absorption spectrum of the sunscreen formulas. Composition and protection factors were given for (**a**) in vitro and (**c**) in vivo studies. The formula absorption spectra were obtained using transmission measurement carried out spectroradiometrically (290–450 nm) through formulas dissolved in ethanol 0.1 g/l. (**b**) The absorption spectra of Reference vitro, Formula vitro 0.7% MCE, and Formula vitro 1.5% MCE were practically superimposed from 290 nm to 350 nm, leading to the close SPF values (between 17 and 20) of the three tested formulations. (**d**) The same results are observed for Reference vivo and Formula vivo 1.5% MCE (SPFs 27 and 32, respectively). Formulas vitro and vivo containing the UVA1 absorbing MCE filter exhibited broader absorption profiles in the UVA1 wavelength range than their respective reference. Fla, formula; MCE, Methoxypropylamino Cyclohexenylidene Ethoxyethylcyanoacetate; PPD, persistent pigment darkening; Ref, reference; SPF, sun-protection factor.

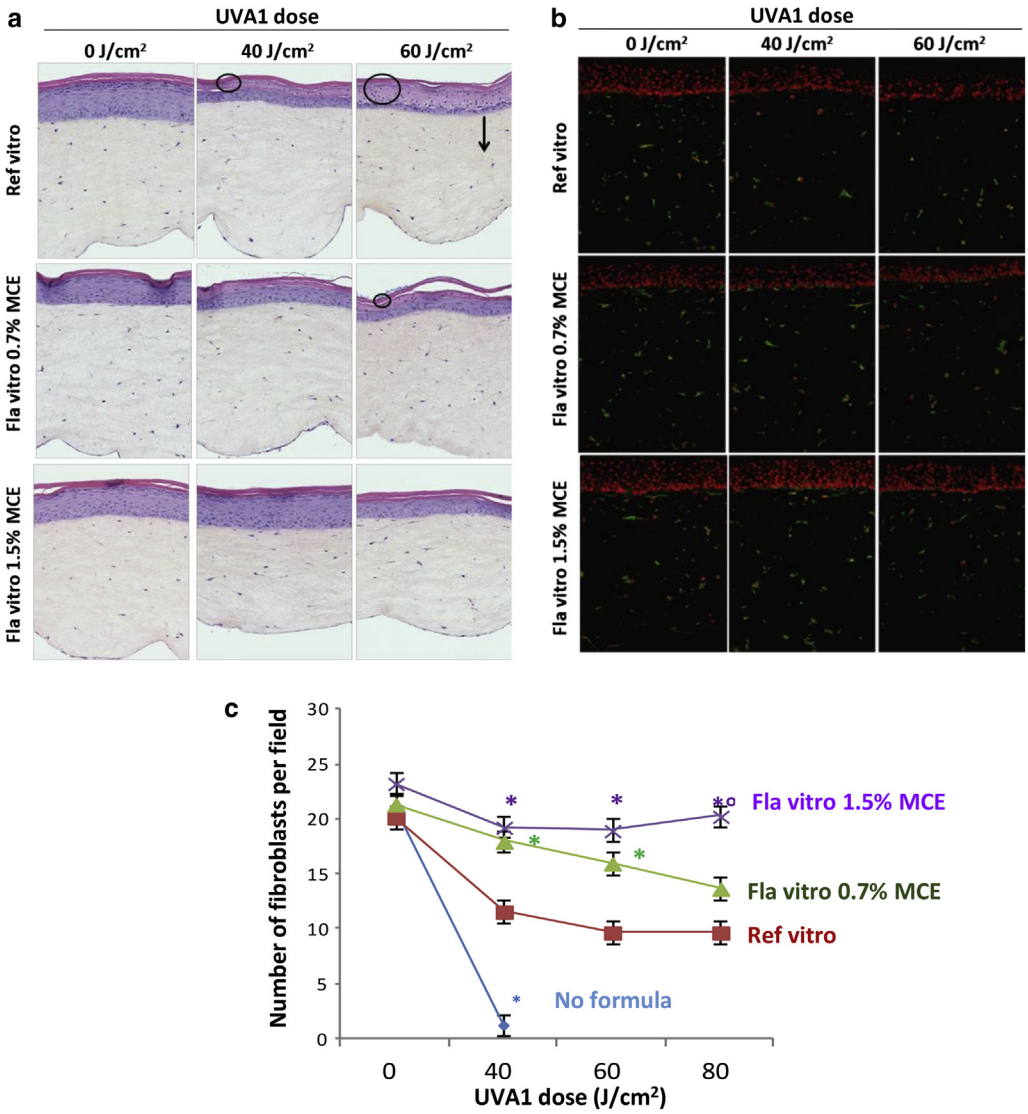

Figure 3. Evaluation of sunscreen formulations on the morphology and number of fibroblasts of reconstructed skins exposed to UVA1. At 48 hours after UVA1 exposure, sections of reconstructed skins were realized to perform (**a**) histology, (**b**) vimentin immunostaining, and (**c**) fibroblasts counting. Four independent experiments were performed. In panel **a**, circles and arrows indicate epidermal alterations and depth of fibroblasts disappearance, respectively. In panel **b**, vimentin staining appears green and is located in fibroblasts' cytoplasm. Cell nuclei counterstained using propidium iodide appear in red. In panel **c**, each point shows the mean value of fibroblasts number per field ± SEM. Asterisk (*) indicates a significant difference from the Reference vitro; degree symbol (°) indicates significant difference from Formula vitro 0.7% MCE (Student's *t*-test, $P < 0.05$). Fla, formula; MCE, Methoxypropylamino Cyclohexenylidene Ethoxyethylcyanoacetate; Ref, reference.

modulation was observed. The Reference vitro enabled the decrease in the number of genes differentially expressed by UVA1 exposure and the intensity of modulation, compared with those in the nonprotected reconstructed skins. The use of Formula vitro 1.5% MCE afforded better protection than the use of Reference vitro on the number and intensity of modulations (Figure 4b). The detailed results for the 27 and 24 genes in fibroblasts and KCs, respectively, are shown in Figures 5 and 6. In fibroblasts, the use of the Reference vitro state-of-the-art formula during UVA1 exposure was sufficient to significantly abrogate the UVA1-induced modulation of five genes: *JUN* oncogene, *APCDD1* apoptosis-related gene, *IL1* proinflammatory gene, *TXNIP* oxidative stress response gene, and *DNAJB1* stress-related gene. Similar to the Reference vitro, Formula vitro 1.5% MCE was also able to protect the UVA1-induced modulation of these genes. In addition, Formula vitro 1.5% MCE significantly reduced the gene expression modulation of *DDIT3* apoptosis gene, *CSF2* inflammation-related gene, *HMOX1* oxidative stress response gene, *HSPA6* stress-related gene, *GDF15* extracellular matrix–related gene, and all the genes of the antiviral response family (*OAS1*, *OAS2*, *MX1*, *MX2*, *IFIT1*, toll-like receptor gene *TLR3*, *DDX58*, *GBP2*, *GBP5*, and *SAMD9*), compared with the Reference vitro. In KCs, Reference vitro enabled to avoid the UVA1-induced gene expression changes of proinflammatory genes (*IL1A*, *CCL20*, and *ICAM1*), gene expression changes of antiviral genes (toll-like receptor gene *TLR3*, *OAS1*, and *OAS2*), and gene expression changes of *NQO1* oxidative stress response gene. Formula vitro 1.5% MCE had the same effect as Reference vitro for these genes but was

Table 4. Evaluation of Sunscreen Formulations on the Levels of Secreted Proteins in Culture Medium of Reconstructed Skins Exposed to UVA1

Amount of Protein in the Condition 0 J/cm^2, No Formula		MMP1 18.3 ± 4.6 ng/ml	IL-1RA 23.0 ± 5.6 ng/ml	IL-6 0.7 ± 0.3 µg/ml	GM-CSF 54.4 ± 13,6 ng/ml	IL-8 2,1 ± 1,2 µg/ml
0 J/cm^2	No formula	1 ± 0.2	1 ± 0.1	1 ± 0.1	1 ± 0.1	1 ± 0.2
40 J/cm^2		**2.7 ± 0.9**	**7.1 ± 2.1**	**2.4 ± 1.0**	**3.3 ± 1.2**	2.7 ± 1.4
40 J/cm^2	Ref vitro	1.2 ± 0.9	6.8 ± 2.1	1.2 ± 1.0	2.4 ± 1.2	1.4 ± 1.4
	Fla vitro 0.7% MCE	1.3 ± 0.3	5.7 ± 1.2	1.4 ± 0.3	2.5 ± 1.1	1.5 ± 0.8
	Fla vitro 1.5% MCE	1.1 ± 0.3	4.0 ± 0.8[1]	1.4 ± 0.6	1.5 ± 0.5	2.3 ± 1.5
60 J/cm^2	Ref vitro	5.6 ± 3.8	33.1 ± 13.0	4.6 ± 3.3	10.9 ± 10.1	5.9 ± 4.7
	Fla vitro 0.7% MCE	1.4 ± 0.5[1]	7.2 ± 2.2[1]	1.3 ± 0.4[1]	2.4 ± 1.1[1]	1.9 ± 0.6[2]
	Fla vitro 1.5% MCE	1.9 ± 0.7[2]	7.4 ± 1.4[1]	2.1 ± 1.0	2.2 ± 0.5[1]	3.1 ± 1.0
80 J/cm^2	Ref vitro	11.1 ± 7.6	76.5 ± 27.6	4.9 ± 2.2	14.2 ± 7.9	6.2 ± 2.3
	Fla vitro 0.7% MCE	3,8 ± 3.1[1]	23.1 ± 18.4[2]	1.9 ± 1.3[1]	6.8 ± 6.5[2]	3.1 ± 1.7[1]
	Fla vitro 1.5% MCE	2.2 ± 1.0[1]	12.6 ± 3.5[1]	1.4 ±- 0.5[1]	3.5 ± 2.3[1]	2.2 ± 0.8[1]

Abbreviations: CI, confidence interval; Fla, formula; MCE, Methoxypropylamino Cyclohexenylidene Ethoxyethylcyanoacetate; MMP1, matrix metalloproteinase 1; Ref, reference.

The amount of secreted proteins was measured 48 hours after UVA1 exposure by ELISA in culture media of reconstructed skins protected or not by a Fla. This was divided by the average number of living fibroblasts. Values of control samples (no UV, no formula) are indicated in the first line and were then adjusted to the 1 value. Values are expressed as means of four independent experiments ± 95% CI. The significant difference between 40 J/cm^2 and 0 J/cm^2 in the absence of formula is reported in bold ($P < 0.05$).

[1]Significant difference from reference vitro ($P < 0.05$).

[2]Significant difference from reference vitro ($0.05 < P < 0.1$) in Student's *t*-test.

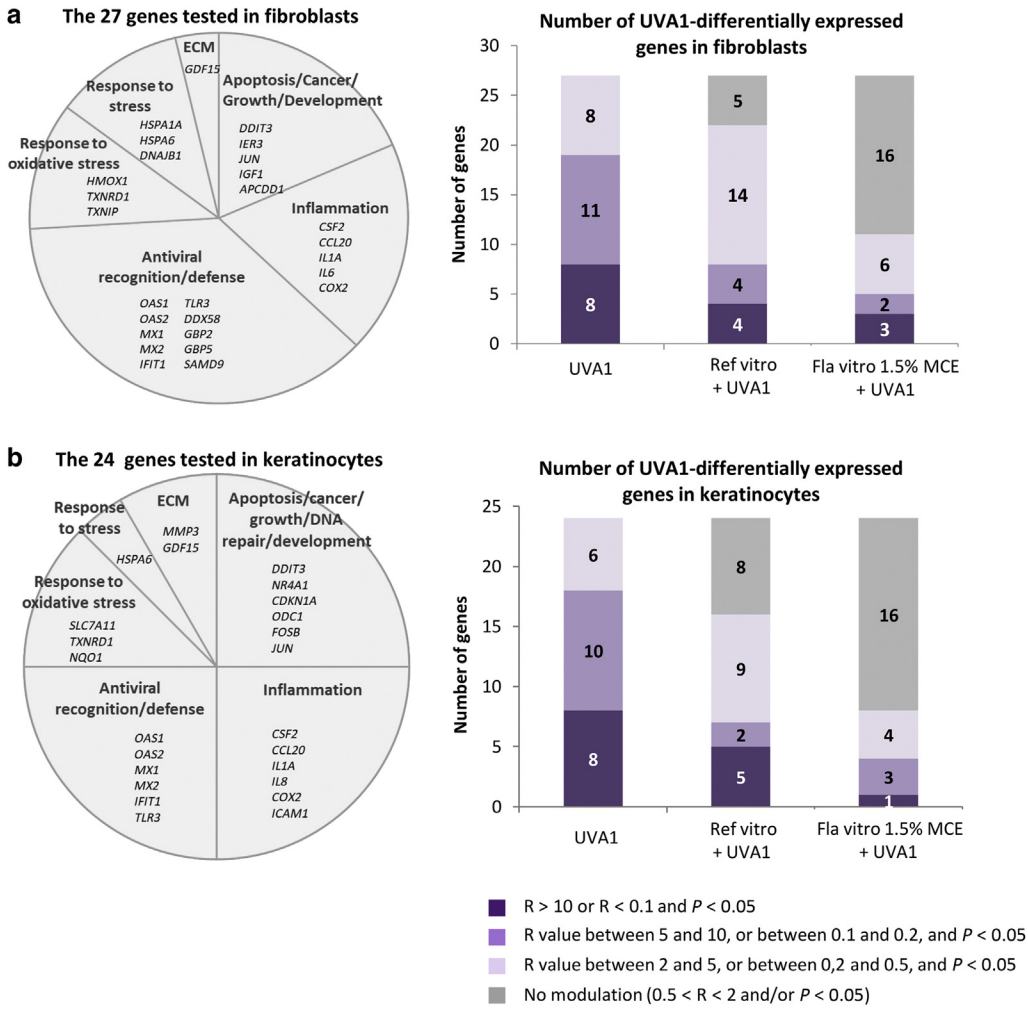

Figure 4. Evaluation of sunscreen formulations on overall gene expression modulations in reconstructed skins exposed to UVA1. Six hours after exposure to 40 J/cm^2 UVA1, the level of 27 and 24 transcripts were measured by qPCR in (**a**) fibroblasts and (**b**) keratinocytes of reconstructed skins, respectively, protected or not by a sunscreen formula. Three independent experiments were performed. Transcripts levels of UVA1-exposed samples were compared with those of nonexposed samples using a Student's *t*-test. A transcript level was considered modulated if the ratio of transcripts level R in UVA1-exposed sample to transcript level in the nonexposed sample was >2 or <0.5 and if the *P*-value was <0.05. Color code gives the intensity of modulation of transcripts level by UVA1. ECM, extracellular matrix; Fla, formula; MCE, Methoxypropylamino Cyclohexenylidene Ethoxyethylcyanoacetate; Ref, reference.

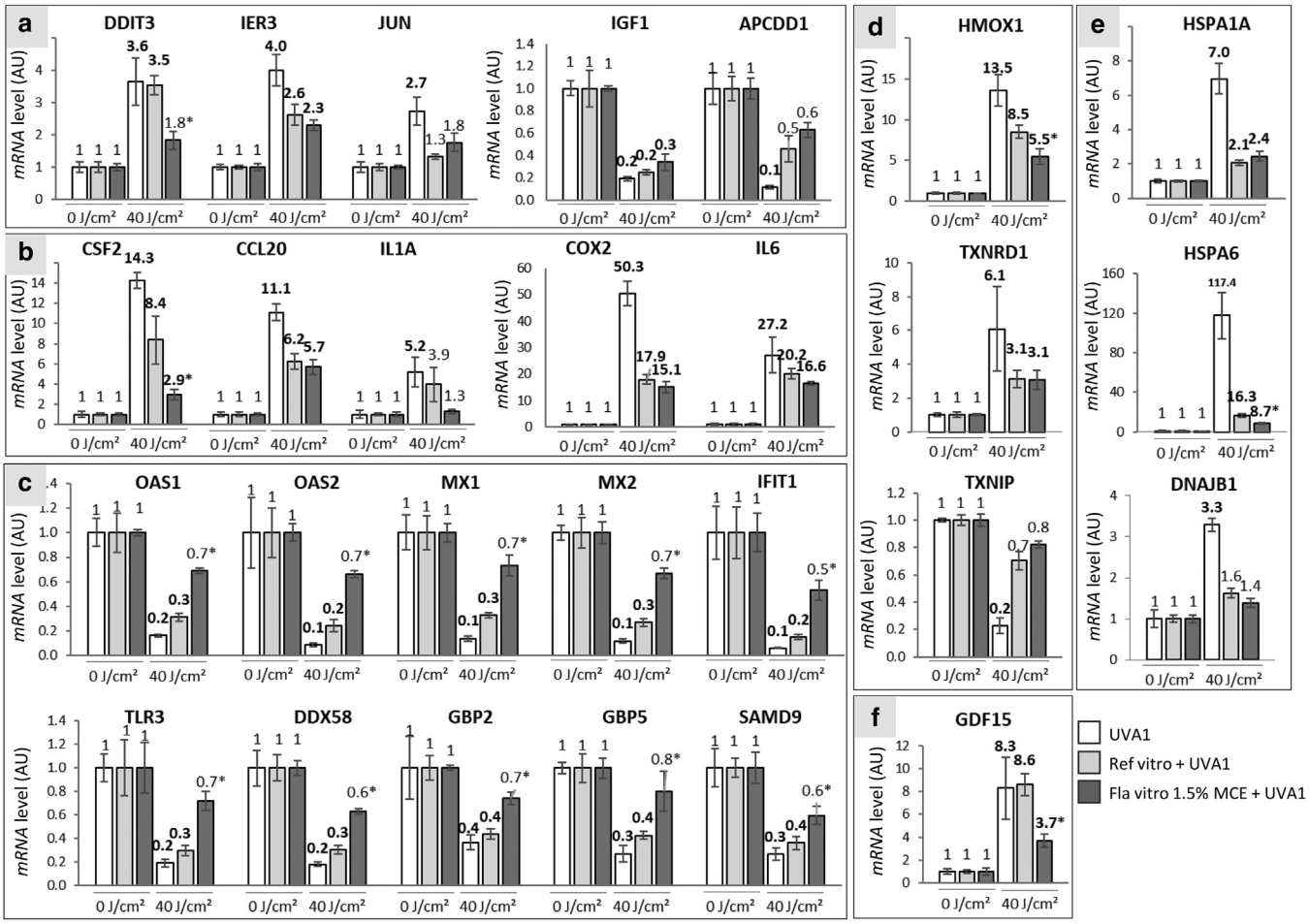

Figure 5. Levels of expression of 27 genes in fibroblasts of reconstructed skins protected or not by a formula and exposed to UVA1. Six hours after exposure to 40 J/cm^2 UVA1, level of transcripts was quantified in a relative manner using qPCR in fibroblasts of the reconstructed skins. Three independent experiments were performed. The studied genes were distributed in the following functional families: (**a**) apoptosis/cancer/growth/development, (**b**) inflammation, (**c**) antiviral recognition/defense, (**d**) response to oxidative stress, (**e**) response to stress, and (**f**) extracellular matrix. White bars indicate nonprotected samples, pale gray bars indicate Reference vitro–protected samples, and dark gray bars indicate Formula vitro 1.5% MCE–protected samples. Each bar shows the mean value ± SEM. Differentially expressed genes are shown in bold versus those of the nonexposed sample. The significant differences between the ratio of Reference vitro–protected and Formula vitro 1.5% MCE–protected samples are indicated by superscript symbols, $^{*}P < 0.05$; $^{\S}0.05 \leq P < 0.1$ (Student's *t*-test). AU, arbitrary unit; MCE, Methoxypropylamino Cyclohexenylidene Ethoxyethylcyanoacetate.

also able to significantly decrease UVA1-induced modulation rates of *NR4A1*, *CDKN1A*, *ODC1*, *FOSB*, *GDF15*, *IFIT1*, *MX2*, *OAS1*, *SLC7A11*, and *TXNRD1*, compared with Reference vitro. Taken together, these results show that the state-of-the-art Reference vitro and Formula vitro 1.5% MCE decreased or abrogated the gene expression modulation induced by UVA1 for most of the studied genes. Formula vitro 1.5% MCE had significantly better protection than Reference vitro against the gene expression modulation induced by UVA1.

The performance of Reference vitro and Formula 1.5% MCE was tested using graphical representation and statistical analysis of the overall gene expression modulation (Figure 7). The biplot visualization allows for a simultaneous representation of the modulation of gene expression and the conditions UVA1, Reference vitro + UVA1, and Formula vitro 1.5% MCE + UVA1. In fibroblasts (Figure 7a) and KCs (Figure 7b), the UVA1 conditions were gathered with all the UVA1-modulated genes (gray and yellow points), except for *HSPA6* in KCs (as detailed in Figure 6). On the first horizontal axis, the Formula vitro 1.5% MCE + UVA1 conditions were located at the opposite of UVA1 conditions, whereas the Reference vitro + UVA1 conditions were located in between. These data show that Reference vitro and Formula vitro 1.5% MCE can protect against the gene expression modulation induced by UVA1 and lead to the following significant ranking in protection efficiency: Formula vitro 1.5% MCE > Reference vitro > no protection ($P = 0.0009$, Jonckheere–Terpstra test).

Altogether, these data show that the addition of the MCE filter in a state-of-the-art formula enabled a better photoprotection of tissue, cellular, biochemical, and molecular changes induced by UVA1 in reconstructed human skin.

In vivo study

Then, a human in vivo study was performed and statistically analyzed in 19 volunteers to compare the photoprotection efficiency of a state-of-the-art formula (Reference vivo), absorbing UVB and UVA up to 370 nm, with that of Formula vivo 1.5% MCE containing 1.5% MCE filter, absorbing UVB

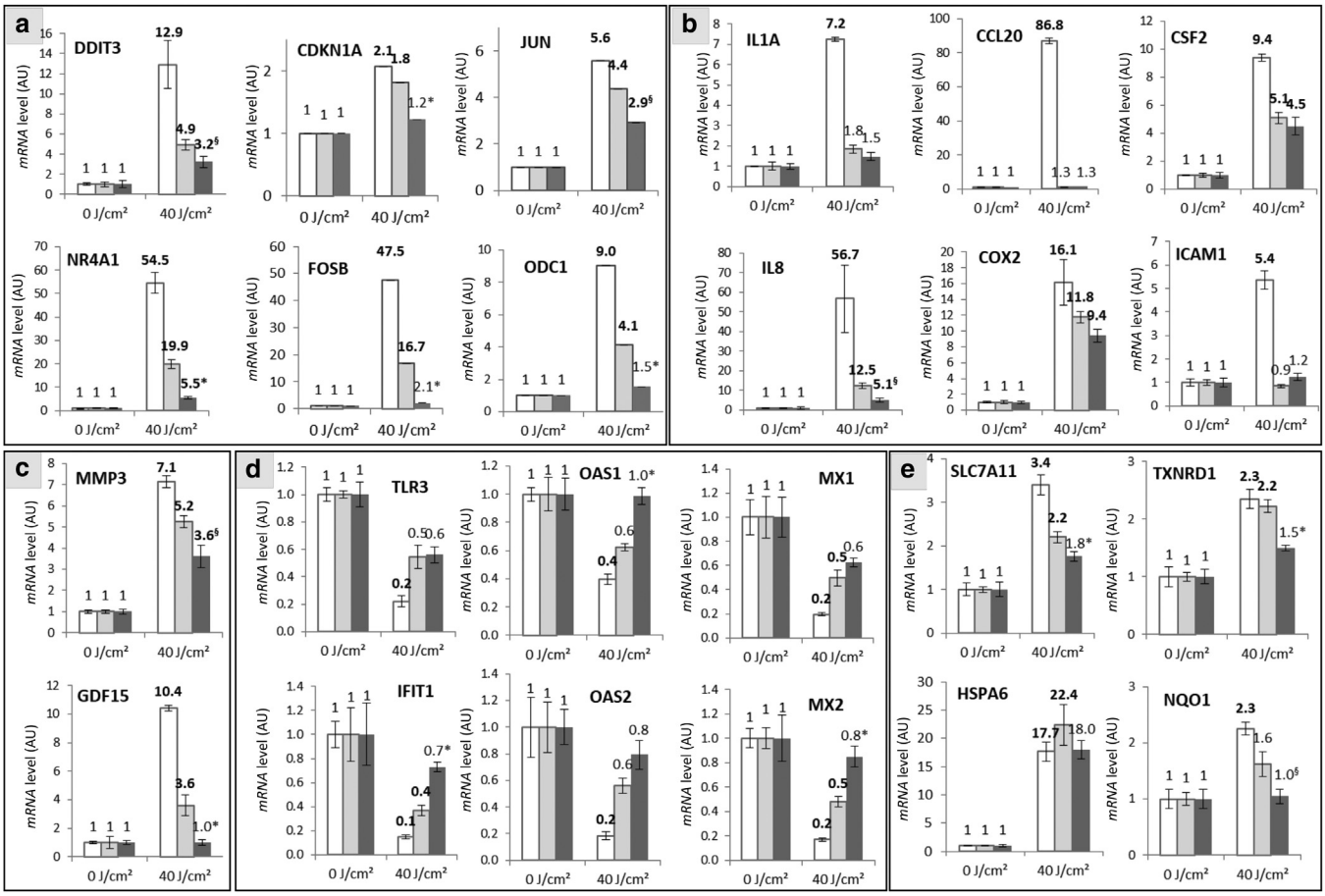

Figure 6. Levels of expression of 24 genes in keratinocytes of reconstructed skins protected or not by a formula and exposed to UVA1. Six hours after exposure to 40 J/cm^2 UVA1, levels of transcripts were quantified in a relative manner using qPCR in keratinocytes of reconstructed skins. Three independent experiments were performed. The studied genes were distributed in the following functional families: (**a**) apoptosis/cancer/growth/DNA repair/development, (**b**) inflammation, (**c**) extracellular matrix, (**d**) antiviral recognition/defense, and (**e**) response to stress/oxidative stress. White bars indicate nonprotected samples, pale gray bars indicate Reference vitro–protected samples, and dark gray bars indicate Formula vitro 1.5% MCE–protected samples. Each bar shows the mean value ± SEM. The differentially expressed genes are shown in bold versus those of the nonexposed sample. The significant differences between the ratio of reference vitro– and formula vitro 1.5% MCE–protected samples are indicated by superscript symbols, $^*P < 0.05$; $^{\S}0.05 \leq P < 0.1$ (Student's *t*-test). AU, arbitrary unit; Fla, formula; MCE, Methoxypropylamino Cyclohexenylidene Ethoxyethylcyanoacetate; Ref, reference.

and UVA up to 400 nm (Figure 2c and d). Both absorption spectra were practically superimposed from 290 nm to 350 nm. Vehicle, Reference vivo, and Formula vivo 1.5% MCE were applied on the back of volunteers before exposure to 50 J/cm^2 UVA1. Chromametry measurements and visual assessment of skin pigmentation were realized before and 2 hours and 24 hours after UVA1 exposure, corresponding to Persistent Pigment Darkening (Moyal et al., 2000; Sklar et al., 2013). As expected, 2 hours after UVA1 exposure, skin darkening of the vehicle-treated zone was induced, with a decrease in skin luminance (ΔL*) and skin color value (Δindividual typology angle [ΔITA°]) and an increase in skin pigmentation (ΔE), compared with that of the nonexposed zone. These changes were maintained 24 hours after UVA1 exposure (Figure 8a). The use of the Reference-vivo-Formula significantly reduced these changes, at both time points. Compared with Reference vivo, Formula vivo 1.5% MCE enabled a significant increase in ΔL* and ΔITA° and a decrease in ΔE, leading to values closer to those of baseline (Figure 8a). Visual assessment on the same tested zones (Figure 8b–d) showed that 2 hours and 24 hours after UVA1 exposure, the vehicle-treated zones presented pigmentation scores between 6 and 10, with 74% of volunteers having a score of 9 or 10 at 2 hours. On the Reference-vivo-formula zone, no more pigmentation score of 10 was observed, the number of volunteers with a score of 9 was drastically reduced, and 5% of the volunteers presented a score of 4. The use of Formula vivo 1.5% MCE reduced even more the number of volunteers with high pigmentation scores and increased the number of volunteers with scores of 4 and 5 (Figure 8b). A statistical analysis on averaged pigmentation scores showed that the use of Reference vivo significantly decreased the mean pigmentation score compared with the use of vehicle and that Formula vivo 1.5% MCE significantly decreased the mean pigmentation score compared with Reference vivo (Figure 8c), as exemplified on the photograph of one subject 24 hours after UVA1 exposure (Figure 8d).

DISCUSSION

The whole UV spectrum (100–400 nm) is classified as carcinogenic to humans by the International Agency for Research on Cancer of the World Health Organization

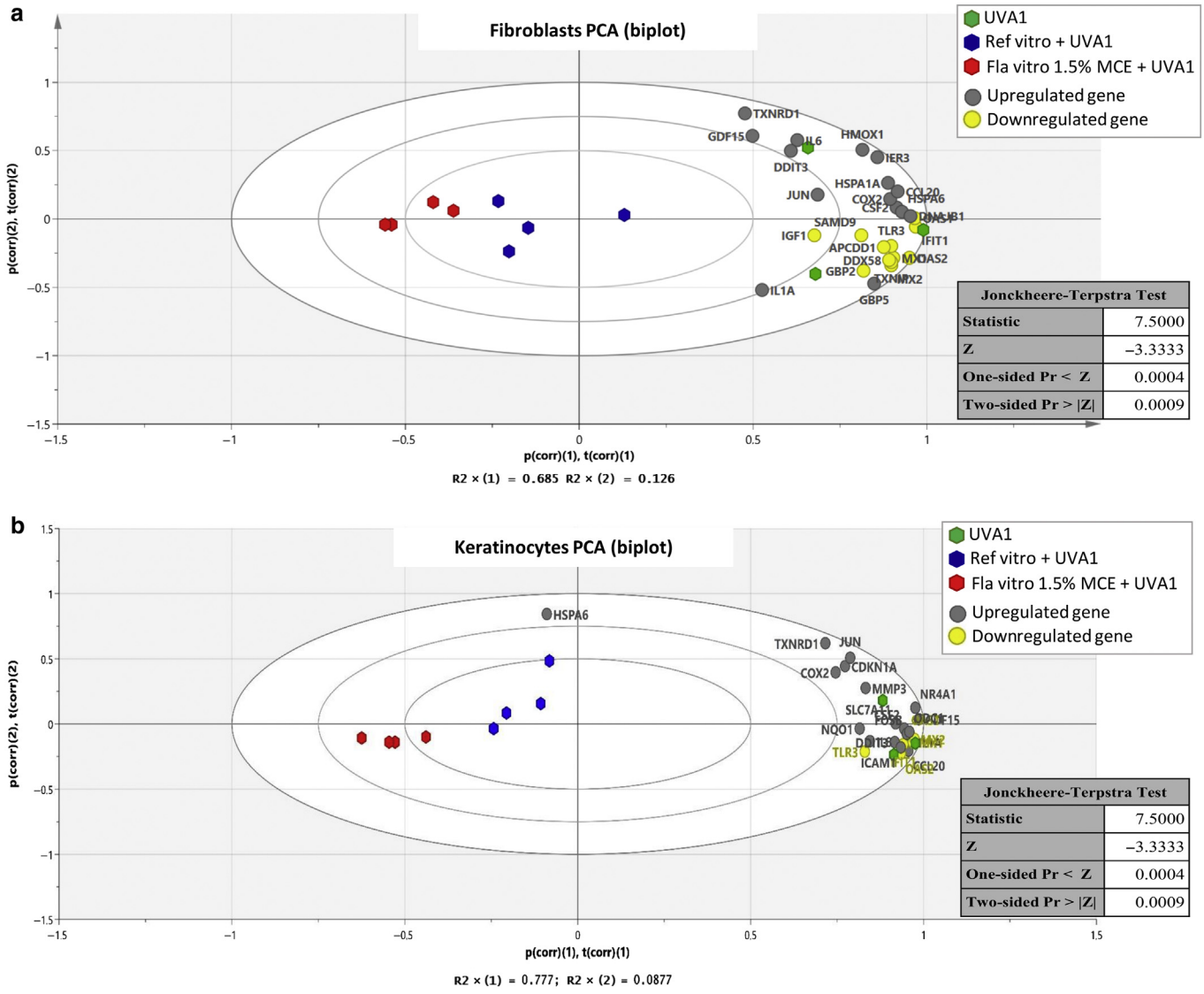

Figure 7. Graphical representation and statistical analysis of the overall gene expression modulation. For (**a**) fibroblasts and (**b**) keratinocytes, the graphic (biplot) displays the first factorial plan of a PCA on the basis of the FC values (R > 1, FC = R; R < 1, FC = 1/R) induced by UVA1 exposure. It shows the similarities and dissimilarities between conditions (UVA1 in green, Reference vitro + UVA1 in blue, and Formula vitro 1.5% MCE + UVA1 in red) and allows for us to interpret these conditions in terms of modulated genes that are also plotted. Upregulated and downregulated genes by UVA1 exposure appear in gray and in yellow, respectively. The results of the associated nonparametric Jonckheere–Terpstra trend test are detailed in the tables. They showed a significant evolution of the scores by conditions ($P = 0.0009$). FC, fold change; Fla, formula; MCE, Methoxypropylamino Cyclohexenylidene Ethoxyethylcyanoacetate; PCA, principal component analysis; Ref, reference.

(International Agency for Research on Cancer, 2012). A growing scientific matter has emphasized the harmful effects of UVA1, the less energetic solar UV wavelengths but representing the largest amount of UV rays reaching the earth. Thanks to the approval by the Scientific Committee on Consumer Safety, the new UVA1 filter, MCE, can now be used in sunscreen products. Owing to its absorption peak at 385 nm, MCE addition in state-of-the-art reference formulas actually enlarged the profile of absorption up to 400 nm.

Using formulas with identical SPFs and similar profiles of absorption up to 370 nm, the efficacy of protection against UVA1 was assessed with or without an MCE filter in the formula.

First, protection was assessed by UVA1-induced epidermal and dermal alterations in a three-dimensional skin model. As expected, under such UVA1 exposure, with realistic doses corresponding to around 2–4 hours of sun exposure depending on latitude and day of the year, the reference sunscreen showed protection of most of the parameters compared with that of unprotected conditions, in line with its absorption profile covering UVA1 up to 370 nm. In this study, on the basis of histological, biochemical, and molecular data, the improvement of protection using formulations containing MCE was demonstrated in a concentration-dependent manner, 1.5% in the formulation being more effective than 0.7%.

UVA1 wavelengths are highly penetrating rays. The protection in the dermis was proven with better protection against dermal fibroblasts alterations and cytokines and MMPs release as well as fibroblastic gene expression

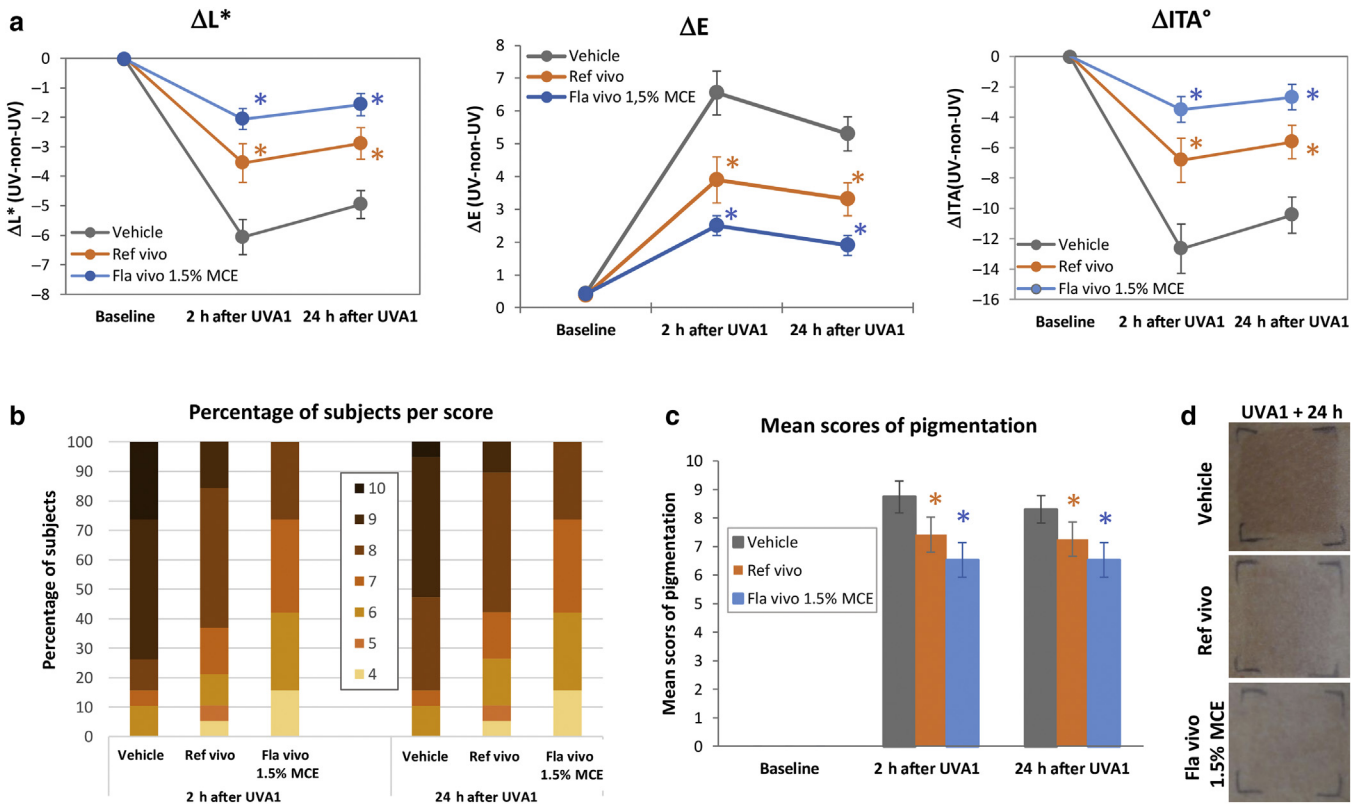

Figure 8. In vivo evaluation of sunscreen formulations on UVA1-induced pigmentation. A total of 2 mg/cm^2 of products were applied per zone onto the back skin of 19 volunteers before UVA1 exposure (50 J/cm^2). Colorimetric parameters (L*, a*, b*) were measured before and 2 h and 24 h after UVA1 exposure. (**a**) Skin luminance (ΔL*), skin pigmentation (ΔE), and ΔITA° between UVA1-exposed and -unexposed zones were calculated for each formula-treated zone. In parallel, a visual pigmentation scoring was performed using a 13-point scale grading from absence (0) to pronounced brown pigmentation (13). The (**b**) percentages of volunteers per score and (**c**) mean scores of pigmentation were plotted. (**d**) A representative photograph 24 h after UVA1 exposure is shown. Values are expressed as means ± 95% CI. Orange and blue asterisks indicate the differences from vehicle and from Reference vivo, respectively ($P < 0.05$). CI, confidence interval; Fla, formula; h, hour; ITA°, individual typology angle; MCE, Methoxypropylamino Cyclohexenylidene Ethoxyethylcyanoacetate; Ref, reference.

modulations, especially those related to oxidative stress, inflammation, and dermal matrix organization. These deep cutaneous impacts have been previously linked to photoaging process and solar elastosis formation (Quan et al., 2009), with a specific role of UVA1 rays (Lavker et al., 1995; Tewari et al., 2014; Wang et al., 2014). These insidious biological alterations have to be taken into account with regard to everyday chronic exposure to UVA1 rays, which are present during most part of the day and less affected by seasons than UVB rays (Jablonski and Chaplin, 2010; Tewari et al., 2013). In that respect, the use of MCE in a daily photoprotection would surely improve, in the long term, the prevention of photoaging signs afforded by sunscreens, as shown in long-term follow-up studies (Hughes et al., 2013; Randhawa et al., 2016).

Molecular data revealed a maintenance of genome expression, as evidenced by the principal component analysis. The selected genes were representative of various biological functions in both cutaneous compartments.

The major mode of action of UVA1 rays is the generation of ROS, leading to subsequent oxidative damage to cellular components such as DNA, lipids, and proteins. This impact has been monitored using the modulation of expression of several target genes of the Nrf2 pathway—*TXNRD1*, *NQO1*, *SLC7A11*, or *HMOX1*—as a sensitive indicator of ROS presence (Gęgotek and Skrzydlewska, 2015). Their expression was upregulated by UVA1 exposure, and in both cell types, the formula containing MCE significantly better prevented this induction than the reference formula (Figures 5 and 6).

UVA1 rays are major contributors to photoimmunosuppression (Damian et al., 2011; Matthews et al., 2010). Their impact is also associated with modulated genes related to innate immunity, with the expression of antiviral defense genes particularly downregulated and inflammation-related markers upregulated (Marionnet et al., 2014). Immune response and antiviral defense are key issues for clinical consequences, such as Herpes simplex virus reactivation or polymorphic light eruptions (Kerr et al., 2012; York and Jacobe, 2010). A competent immune response is also mandatory in the prevention of skin carcinogenesis, both innate and adaptive immunity participating in tumor immunosurveillance and antitumor effects (Jakóbisiak et al., 2003; Valejo Coelho et al., 2016; Yu et al., 2014). This study showed that MCE addition in sunscreen formulation can significantly improve photoprotection compared with the reference, with most genes related to immunity having their gene expression normalized using MCE.

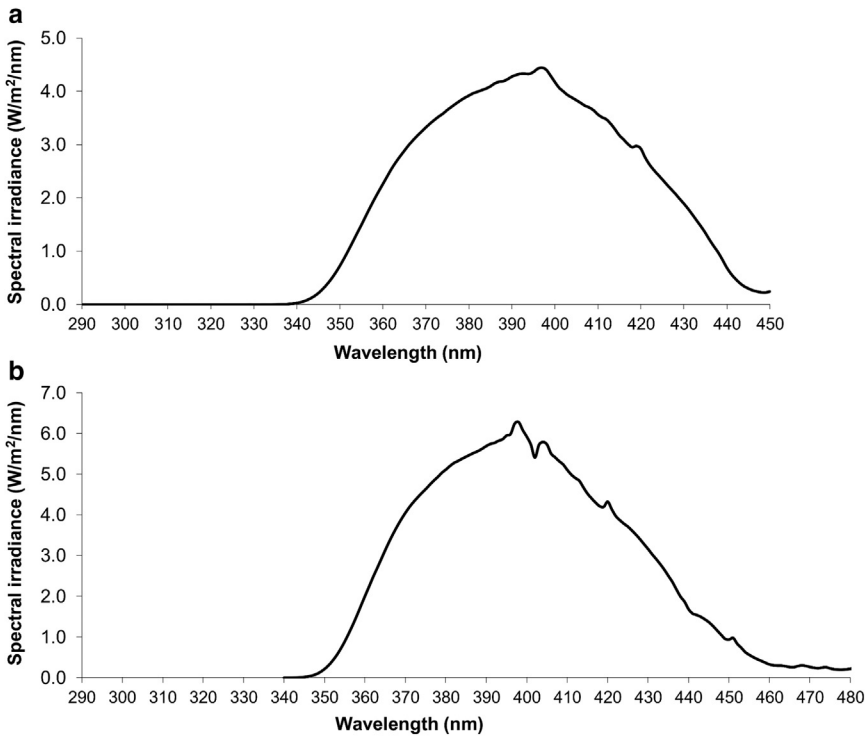

Figure 9. UVA1 emission spectra. In the (**a**) in vitro and (**b**) in vivo studies, UVA1 rays were delivered using an Oriel solar simulator (1,000 W and 1,600 W, respectively) equipped with a dichroic mirror and a WG360 2 mm thick filter. Emission spectra were recorded using a calibrated Macam spectroradiometer. To deliver all of the UVA1 wavelengths (up to 400 nm), a part of the visible light spectrum (400–450 nm) could not be separated from applied UVA spectra of wavelengths.

In addition, other genes important in the fate of KCs, the cells at the origin of carcinomas, have their expressions less perturbated when the sunscreen protection is enlarged by adding MCE: notably, the transcription factors *NR4A1*, exhibiting growth-promoting, angiogenic, and prosurvival activity in most cancers; *DDIT3* (*CHOP/GADD153*) inducible in KCs by genotoxic stress and growth arrest signals such as UV exposure, whose upregulation reflects endoplasmic reticulum stress (Garmyn et al., 1995; Oyadomari and Mori, 2004); and also *JUN* and *FOSB* oncogenes. Moreover, the induction by UVA1 of *CDKN1A* gene, encoding p21Cip1/Waf1 involved in cell cycle arrest to allow DNA repair after DNA damage (Al Bitar and Gali-Muhtasib, 2019), was completely abolished with the use of the formulation containing 1.5% MCE. This could reflect the protection from UVA1-induced DNA damage afforded by the addition of MCE in sunscreens. Altogether, these results are, to our knowledge, previously unreported preliminary biological evidence suggesting a benefit of MCE-containing sunscreen products in UV-induced cancer prevention.

Evaluation of clinical consequences, especially those requiring long-term exposures, is a difficult issue. In this study, the pigmentation corresponding to the Persistent Pigment Darkening was used as a clinical surrogate for the impact of UVA1 exposure because we previously showed that this pigmentation was associated with biological alterations related to inflammation, response to oxidative stress, perturbation of extracellular matrix, cancer, and development (Marionnet et al., 2017). These effects were achieved after exposure to 50 J/cm^2 UVA1, the same dose as in this study. Such UVA1 dose can be received in <3 hours in summer. In this study, topical application of sunscreens formulations led to a decrease in the level of UVA1-induced pigmentation, with higher prevention of pigmentation when the sunscreen contained 1.5% MCE. On the basis of absorption profiles of both sunscreen formulations, the gain of efficacy of sunscreen containing MCE is attributed to its filtering properties in the 370–400 nm wavelengths range. Because only short-time effects have been assessed through Persistent Pigment Darkening, complementary studies will be engaged to better assess the delayed tanning at longer time points. Although no melanocytes were comprised in the in vitro skin model, making the analysis of direct actors of melanogenesis not possible, some KCs and fibroblasts factors known to contribute to UV-induced pigmentation such as CSF2/GM-CSF, which activates UVA-induced melanogenesis (Imokawa et al., 1996), and GDF15, which has recently been shown to stimulate melanogenesis through MITF/tyrosinase upregulation (Kim et al., 2020), had their mRNA levels significantly normalized when the MCE formulation was used compared with those of the reference formulation.

For the first time, thanks to MCE filtering properties, a full coverage of the whole UV spectrum up to 400 nm was reached, leading to a higher photoprotection against UVA1-induced biological and clinical impacts. The data strongly support the benefits in the long term on sun-induced consequences, especially those related to public healthcare issues. Additional clinical studies should expand proofs of efficacy.

MATERIALS AND METHODS

UVA1 sources

Solar simulators (Oriel, Stratford, CT) with a 1,600 W (in vivo study) or a 1,000 W (in vitro study) Xenon lamp equipped with a dichroic mirror (Oriel, Les Ulis, France) + WG360 2 mm thick filter (Schott, Clichy, France) delivered the so-called UVA1 spectrum (340–450 nm) (Marionnet et al., 2014) (Figure 9).

MCE UVA1 filter

The MCE UVA1 filter (International Union of Pure and Applied Chemistry name: 2-ethoxyethyl (2Z)-2-cyano-2-[3-(3-methoxypropylamino) cyclohex-2-en-1- ylidene]acetate; CAS number 1419401-88-9) belongs to the cyclic merocyanine family (Winkler et al., 2014) and has a 322.41 g/mol molecular weight (Figure 1).

Sunscreen products

State-of-the-art formulas were used as references. Formulas vitro 0.7% MCE and Formula vitro 1.5% MCE, containing 0.7 and 1.5% MCE, respectively, were used in vitro. Formula vivo 1.5% MCE, containing 1.5% MCE, was used in vivo. Figure 2 details the formulas compositions, protection factors, and absorption spectra. Owing to formulations' technical constraints (filters compatibility and stability), the composition of the SPF15 formulas for in vitro studies and SPF30 formulations for in vivo clinical trial requested specific adjustments in their compositions.

In vitro study

In vitro reconstructed skin model. Normal primary KCs and fibroblasts were isolated from normal human skin as described (Bernerd and Asselineau, 1997). Human skin was obtained from surgical residues after written informed consent from the donors according to the principles expressed in the Declaration of Helsinki and in article L.1243-4 of the French Public Health Code. Reconstructed skins were composed of a dermal equivalent embedding human living dermal fibroblasts, overlaid by an epidermis reconstructed with human epidermal KCs, as previously described (Bernerd and Asselineau, 1997).

In vitro sunscreen application and UVA1 exposure. A total of 2 mg/cm^2 of sunscreen formula were topically applied onto reconstructed skin samples. Five minutes later, the reconstructed skins were exposed to a single UVA1 dose. During this exposure, Dulbecco's phosphate-buffered saline without calcium and magnesium (Gibco BRL, Grand Island, NY) medium was used. After exposure, phosphate-buffered saline was replaced by a fresh medium, and reconstructed skin samples were incubated at 37 °C in 5% carbon dioxide for different time periods, depending on the further performed test.

Morphology and fibroblasts counting. Samples were taken and fixed in neutral formalin for histology 48 hours after UVA1 exposure. Histological examination was performed on paraffin sections stained with hematoxylin, eosin, saffron. Fibroblasts were counted using ImageJ software (National Institutes of Health, Bethesda, MA; http://rsb.info.nih.gov/ij/). For each replicate of one condition, six fields were counted. Then, for one condition, the number of counted fibroblasts per replicate was averaged.

Measurement of protein amount (ELISA). The amount of secreted proteins in the culture medium was measured using ELISA 48 hours after UVA1 exposure. MMP1 amount was assessed using Amersham MMP-1 Human Biotrak assay (GE Healthcare, Chalfont St Giles, United Kingdom). Amounts of IL-1RA, IL-6, IL-8, and GM-CSF were simultaneously assessed using the MILLIPLEX Immunology Multiplex Assay HCYTOMAG-60K (Merck, Darmstadt, Germany) according to manufacturer's instructions and were divided by the average number of fibroblasts seen in paraffin sections, as described earlier, to take into account dermal fibroblast number.

Total RNA extraction. Six hours after UVA1 exposure, reconstructed skin samples were rinsed in Dulbecco's phosphate-buffered saline without calcium and magnesium (Gibco BRL). As previously described, the epidermis was separated from the dermis, and each skin compartment was disrupted and treated with proteinase K. Then, total RNA was extracted from epidermal and dermal samples (Marionnet et al., 2006). The quality of total RNA was analyzed using a 2100 Bioanalyzer and RNA Nanochips (Agilent Technologies, Santa Clara, CA). The amount of total RNA was measured using a Nanodrop ND-1000 spectrophotometer (Thermo Fisher Scientific, Waltham, MA).

Quantitative reverse transcription-polymerase chain reaction (RT-qPCR). First-strand cDNA synthesis was performed using 1 μg of total RNA and the Advantage RT-for-PCR kit (Clontech, Saint Quentin en Yvelines, France). The LightCycler 480 and the LightCycler-FastStart DNA Master SYBR Green kit (F. Hoffmann-La Roche, Basel, Switzerland) were used for qPCR), as previously described (Marionnet et al., 2006). Normalization of mRNA amounts was done using Genorm application and the following housekeeping genes: *GAPDH*, *B2M*, *RPL13A*, *RPS28*, and *RPS9* (Savli et al., 2003; Vandesompele et al., 2002).

Immunostaining. At 48 hours after exposure, immunostaining of vimentin was performed on air-dried vertical 5 μm cryosections using mouse mAb against human vimentin (1:20, Monosan, Unden, The Netherlands). FITC-conjugated rabbit anti-mouse immunoglobulins (1:80, Dako, Glostrup, Denmark) were used as a second antibody. Nuclear counterstaining using propidium iodide was carried out routinely.

Statistical analysis. Fibroblasts number and mean secreted protein amounts were compared using a Student's *t*-test. For gene expression, the level of normalized transcripts was compared between nonexposed and exposed samples in the conditions UVA1, Reference vitro + UVA1, and Formula vitro 1.5% MCE + UVA1 using a Student's *t*-test. A transcript level was considered as modulated by UVA1 exposure when the R modulation ratio of UVA1-exposed sample to nonexposed sample was >2 or <0.5 and significantly different ($P < 0.05$).

For the overall comparisons of conditions UVA1, Reference vitro + UVA1, and Formula vitro 1.5% MCE + UVA1, the values of the fold change (FC) were calculated as follows: for $R > 1$, $FC = R$; for $R < 1$, $FC = 1/R$. Then, a biplot displaying the first factorial plan of a principal component analysis on the basis of the FC values was carried out. A nonparametric Jonckheere–Terpstra trend test was performed on the first principal component to test the evolution of the FC, depending on conditions.

In vivo study

The full protocol and clinical study report are available at L'Oréal Research Center (Aulnay-sous-Bois, France).

Inclusion and noninclusion criteria. Healthy European volunteers aged 18–40 years with Fitzpatrick phototypes III–IV and ITA° ranging from 10° to 35° were recruited. Volunteers without any history of abnormal response to the sun; with no UV tanning marks, freckles, nevi on the back; and without any marks of recent suntan episode were selected. They were requested not to expose themselves to solar or artificial UV sources during the entire study duration.

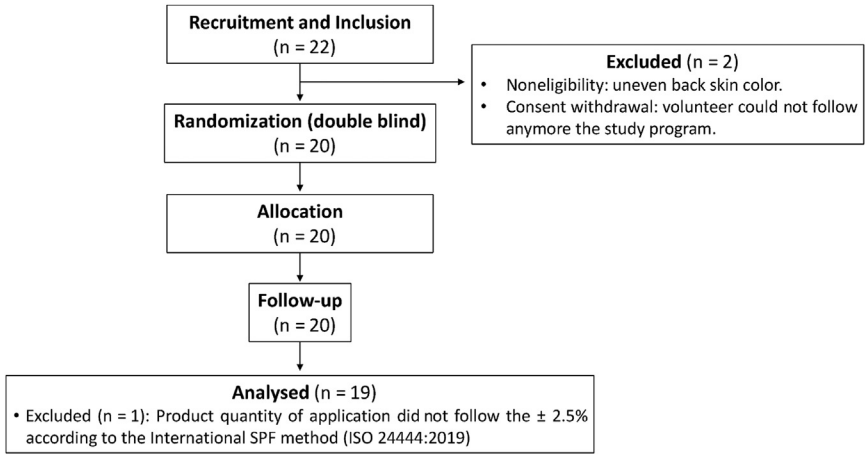

Figure 10. CONSORT flow diagram of the clinical trial. A total of 22 volunteers were included in the study. Two of them were excluded for noneligibility and consent withdrawal reasons. A total of 20 randomized volunteers finalized the study, and one of them was excluded from the statistical analysis owing to an issue related to the application quantity of the product. Therefore, the data analysis was performed on 19 volunteers. CONSORT, Consolidated Standards of Reporting Trials; ISO, International Organization for Standardization; SPF, sun-protection factor.

Demography. A total of 20 volunteers were included, 10 women and 10 men. A total of 10 volunteers were classified as Fitzpatrick phototype III, and 10 were classified as Fitzpatrick phototype IV. The ITA° mean of the panel was 23.5°. The panel mean age was 27.85 years, and the median age was 27.5 years.

Protocol. The study was in accordance with the Helsinki Declaration, approved by the Romanian Health Department on 16 December 2013 with registration number N°77373/16.12.2013, and conducted at the investigational site CIDP Biotechnology SRL (Bucharest, Romania) from 31 January 2014 to 20 February 2014. All enrolled volunteers gave their written informed consent.

The study was monocentric, double-blinded, randomized, and comparative; each subject was their own control. The is registered under the ClinicalTrials.gov identification number NCT04865094.

A total of 2 mg/cm^2 of formulas (vehicle, Reference vivo, or Formula vivo 1.5% MCE) were applied on three zones of 3 × 3 cm^2 on the volunteers' back before exposure to 50 J/cm^2 UVA1. Pigmentation was assessed before and 2 hours and 24 hours after UVA1 exposure.

Assignment and masking. The sample size estimation (20 subjects) was performed by a statistician on the basis of a previous study comparing sunscreen formulas under the same UVA1 exposure condition and with similar colorimetric measurements (Marionnet et al., 2018).

At the Day 1 (baseline), each subject fulfilling all inclusion criteria was assigned a randomization number (provided by L'Oréal Research through an electronic case report form) in the chronological order of inclusion. No number was omitted or skipped. The three zones were delimited on the right or left side of the back of the volunteers and were pretreated with vehicle or the two tested formulas in a randomized manner before exposure to UVA1.

Randomization. Randomization list was generated by a computer process before the study by L'Oréal Research and integrated into the electronic case report form. Randomization numbers were attributed to the volunteers following the distribution indicated by the randomization list. The investigator was supplied with sealed envelopes provided by L'Oréal Research for each subject randomization number with information of the formulas (vehicle, Reference vivo, or Formula vivo 1.5% MCE) assignment to each investigational zone. Only in case of safety concerns (local intolerance, adverse event, serious adverse event) was the investigator authorized to open the corresponding envelope. In this case, the volunteer was in major deviation and was excluded from analysis.

Participant flow and follow-up. The 20 randomized volunteers were followed up for 2 and 24 hours after UVA1 exposure and finalized the study. One volunteer was excluded from the statistical analysis owing to the product quantity of application that did not follow the ±2.5% according to the international SPF method (ISO 24444:2019). As a consequence, the data analysis was performed on 19 volunteers (Figure 10).

Safety concerns. No local intolerance, serious adverse events, or adverse events were reported during the study.

Analysis. For colorimetric measurements, a chromameter (CR300, Konica Minolta, Tokyo, Japan) was used to determine L*, a*, b*. Skin color was characterized by the ITA: ITA° = ArcTangent ([L*−50)/b*])180/π (Del Bino et al., 2013). The primary criterion was the induced pigmentation (ΔE), between the UVA1-exposed zones and their unexposed adjacent zones, calculated as follows: $\Delta E = \sqrt{(\Delta L^2 + \Delta a^2 + \Delta b^2)}$.

For visual scoring of skin pigmentation, visual pigmentation assessment was done under standard daylight illumination on each exposed zone using a pigmentation scale, grading from 0 (absence of pigmentation) to 13 (pronounced brown pigmentation) (Marionnet et al., 2018).

For statistical analysis, chromametric measurements and clinical grading were statistically analyzed in 19 volunteers using linear mixed models for repeated longitudinal data, with treatment, time, and the interaction treatment X time as fixed factors, the baseline as the covariate, and the subject as a random factor. All within- and between-treatment group comparisons were performed using contrasts on the basis of *t*-tests. Adjustments for multiple comparisons were carried out using the Benjamini–Hochberg procedure. Statistical analyses were carried out using SAS 9.3 software (SAS Institute, Cary, NC). The two-sided significance threshold was set at 5%.

Data availability statement

This paper does not include large-scale databases (next-generation sequencing or microarray). However, all data generated during and/or analyzed during these studies are available from the corresponding author on reasonable request.

ORCIDs
Claire Marionnet: http://orcid.org/0000-0003-2474-2001
Romain de Dormael: http://orcid.org/0000-0001-7160-0570
Xavier Marat: http://orcid.org/0000-0002-6709-5695
Angélina Roudot: http://orcid.org/0000-0003-0801-352X
Julie Gizard: http://orcid.org/0000-0003-1265-1858
Emilie Planel: http://orcid.org/0000-0002-0119-9467
Carine Tornier: http://orcid.org/0000-0001-9589-3734
Christelle Golebiewski: http://orcid.org/0000-0003-1827-4571
Philippe Bastien: http://orcid.org/0000-0002-5602-5827
Didier Candau: http://orcid.org/0000-0003-4369-8878
Françoise Bernerd: http://orcid.org/0000-0001-5426-7948

AUTHOR CONTRIBUTIONS
Conceptualization: CM, RDD, DC, FB; Data Curation: CM, RDD, EP, PB; Formal Analysis: PB; Investigation: RDD, JG, CT, CG; Methodology: XM, AR, DC; Supervision: DC, FB; Validation: CM, RDD, EP; Visualization: CM, FB; Writing – Original Draft Preparation: CM, FB; Writing – Review and Editing: CM, RDD, XM, AR, EP, CT, PB, DC, FB

CONFLICT OF INTEREST
CM, RDD, XM, AR, JG, EP, CG, PB, DC, and FB are employees of L'Oréal Research and Innovation, Aulnay-sous-Bois and Chevilly-Larue, France (a cosmetic manufacturer that commercializes sunscreens). CT is an employee of Episkin (Lyon, France).

ACKNOWLEDGMENTS
The authors thank Safa Ben Hassine for technical assistance and Diane-Lore Vieu for artwork.

REFERENCES

Al Bitar S, Gali-Muhtasib H. The role of the cyclin dependent kinase inhibitor $p21^{cip1/waf1}$ in targeting cancer: molecular mechanisms and novel therapeutics. Cancers 2019;11:1475.

Badri T, Schlessinger J. Solar urticaria. In: StatPearls [internet]. Treasure Island, FL: StatPearls Publishing; 2020.

Bernerd F, Asselineau D. Successive alteration and recovery of epidermal differentiation and morphogenesis after specific UVB-damages in skin reconstructed in vitro. Dev Biol 1997;183:123–38.

Daly S, Ouyang H, Maitra P. Chemistry of sunscreens. In: Wang SQ, Lim HW, editors. Principles and practice of photoprotection. Cham, Switzerland: Springer International Publishing; 2016. p. 159–78.

Damian DL, Matthews YJ, Phan TA, Halliday GM. An action spectrum for ultraviolet radiation-induced immunosuppression in humans. Br J Dermatol 2011;164:657–9.

de Laat A, van der Leun JC, de Gruijl FR. Carcinogenesis induced by UVA (365-nm) radiation: the dose-time dependence of tumor formation in hairless mice. Carcinogenesis 1997;18:1013–20.

Del Bino S, Sok J, Bernerd F. Assessment of ultraviolet-radiation-induced DNA damage within melanocytes in skin of different constitutive pigmentation. Br J Dermatol 2013;168:1120–3.

Dennis LK, Vanbeek MJ, Beane Freeman LE, Smith BJ, Dawson DV, Coughlin JA. Sunburns and risk of cutaneous melanoma: does age matter? A comprehensive meta-analysis. Ann Epidemiol 2008;18:614–27.

Gandini S, Autier P, Boniol M. Reviews on sun exposure and artificial light and melanoma. Prog Biophys Mol Biol 2011;107:362–6.

Garmyn M, Degreef H, Gilchrest BA. The effect of acute and chronic photodamage on gene expression in human keratinocytes. Dermatology 1995;190:305–8.

Gęgotek A, Skrzydlewska E. The role of transcription factor Nrf2 in skin cells metabolism. Arch Dermatol Res 2015;307:385–96.

Gibbs NK, Norval M. Photoimmunosuppression: a brief overview. Photodermatol Photoimmunol Photomed 2013;29:57–64.

Hughes MC, Williams GM, Baker P, Green AC. Sunscreen and prevention of skin aging: a randomized trial. Ann Intern Med 2013;158:781–90.

Imokawa G, Yada Y, Kimura M, Morisaki N. Granulocyte/macrophage colony-stimulating factor is an intrinsic keratinocyte-derived growth factor for human melanocytes in UVA-induced melanosis. Biochem J 1996;313:625–31.

International Agency for Research on Cancer. I. A review of human carcinogens. Radiation. 100D. Lyon, FR: WHO Press; 2012.

Jablonski NG, Chaplin G. Colloquium paper: human skin pigmentation as an adaptation to UV radiation. Proc Natl Acad Sci USA 2010;107(Suppl. 2):8962–8.

Jakóbisiak M, Lasek W, Gołab J. Natural mechanisms protecting against cancer. [Published correction appears in Immunol Lett 2004;91:255]. Immunol Lett 2003;90:103–22.

Kerr AC, Ferguson J, Attili SK, Beattie PE, Coleman AJ, Dawe RS, et al. Ultraviolet A1 phototherapy: a British Photodermatology Group workshop report. Clin Exp Dermatol 2012;37:219–26.

Kim Y, Kang B, Kim JC, Park TJ, Kang HY. Senescent fibroblast-derived GDF15 induces skin pigmentation. J Invest Dermatol 2020;140:2478–86.e4.

Lavker RM, Gerberick GF, Veres D, Irwin CJ, Kaidbey KH. Cumulative effects from repeated exposures to suberythemal doses of UVB and UVA in human skin. J Am Acad Dermatol 1995;32:53–62.

Lembo S, Raimondo A. Polymorphic light eruption: what's new in pathogenesis and management. Front Med (Lausanne) 2018;5:252.

Ley RD, Fourtanier A. UVAI-induced edema and pyrimidine dimers in murine skin. Photochem Photobiol 2000;72:485–7.

Marionnet C, Nouveau S, Hourblin V, Pillai K, Manco M, Bastien P, et al. UVA1-induced skin darkening is associated with molecular changes even in highly pigmented skin individuals. J Invest Dermatol 2017;137:1184–7.

Marionnet C, Pierrard C, Golebiewski C, Bernerd F. Diversity of biological effects induced by longwave UVA rays (UVA1) in reconstructed skin. PLoS One 2014;9:e105263.

Marionnet C, Pierrard C, Vioux-Chagnoleau C, Sok J, Asselineau D, Bernerd F. Interactions between fibroblasts and keratinocytes in morphogenesis of dermal epidermal junction in a model of reconstructed skin. J Invest Dermatol 2006;126:971–9.

Marionnet C, Tran C, Bastien P, Bielicki A, Golebiewski C, Vieu DL, et al. A broader filtration of UVA1 wavelengths improves skin photoprotection. J Dermatol Sci 2018;91:337–40.

Matthews YJ, Halliday GM, Phan TA, Damian DL. Wavelength dependency for UVA-induced suppression of recall immunity in humans. J Dermatol Sci 2010;59:192–7.

Milon A, Bulliard JL, Vuilleumier L, Danuser B, Vernez D. Estimating the contribution of occupational solar ultraviolet exposure to skin cancer. Br J Dermatol 2014;170:157–64.

Moyal D. Need for a well-balanced sunscreen to protect human skin from both ultraviolet A and ultraviolet B damage. Indian J Dermatol Venereol Leprol 2012;78(Suppl. 1):S24–30.

Moyal D, Chardon A, Kollias N. Determination of UVA protection factors using the persistent pigment darkening (PPD) as the end point. (Part 1). Calibration of the method. Photodermatol Photoimmunol Photomed 2000;16:245–9.

Ortonne JP. Pigmentary changes of the ageing skin. Br J Dermatol 1990;122(Suppl. 35):21–8.

Oyadomari S, Mori M. Roles of CHOP/GADD153 in endoplasmic reticulum stress. Cell Death Differ 2004;11:381–9.

Quan T, Qin Z, Xia W, Shao Y, Voorhees JJ, Fisher GJ. Matrix-degrading metalloproteinases in photoaging. J Investig Dermatol Symp Proc 2009;14:20–4.

Randhawa M, Wang S, Leyden JJ, Cula GO, Pagnoni A, Southall MD. Daily use of a facial broad spectrum sunscreen over one-year significantly improves clinical evaluation of photoaging. Dermatol Surg 2016;42:1354–61.

Ravnbak MH, Wulf HC. Pigmentation after single and multiple UV-exposures depending on UV-spectrum. Arch Dermatol Res 2007;299:25–32.

Rittié L, Fisher GJ. Natural and sun-induced aging of human skin. Cold Spring Harb Perspect Med 2015;5:a015370.

Rünger TM, Farahvash B, Hatvani Z, Rees A. Comparison of DNA damage responses following equimutagenic doses of UVA and UVB: a less effective cell cycle arrest with UVA may render UVA-induced pyrimidine dimers more mutagenic than UVB-induced ones. Photochem Photobiol Sci 2012;11:207–15.

Savli H, Karadenizli A, Kolayli F, Gundes S, Ozbek U, Vahaboglu H. Expression stability of six housekeeping genes: a proposal for resistance gene quantification studies of Pseudomonas aeruginosa by real-time quantitative RT-PCR. J Med Microbiol 2003;52:403–8.

Sklar LR, Almutawa F, Lim HW, Hamzavi I. Effects of ultraviolet radiation, visible light, and infrared radiation on erythema and pigmentation: a review. Photochem Photobiol Sci 2013;12:54–64.

Tewari A, Grage MM, Harrison GI, Sarkany R, Young AR. UVA1 is skin deep: molecular and clinical implications. Photochem Photobiol Sci 2013;12:95–103.

Tewari A, Grys K, Kollet J, Sarkany R, Young AR. Upregulation of MMP12 and its activity by UVA1 in human skin: potential implications for photoaging. J Invest Dermatol 2014;134:2598–609.

Valejo Coelho MM, Matos TR, Apetato M. The dark side of the light: mechanisms of photocarcinogenesis. Clin Dermatol 2016;34:563–70.

Vandesompele J, De Preter K, Pattyn F, Poppe B, Van Roy N, De Paepe A, et al. Accurate normalization of real-time quantitative RT-PCR data by geometric averaging of multiple internal control genes. Genome Biol 2002;3: RESEARCH0034.

Verkouteren JAC, Ramdas KHR, Wakkee M, Nijsten T. Epidemiology of basal cell carcinoma: scholarly review. Br J Dermatol 2017;177:359–72.

Wang F, Smith NR, Tran BA, Kang S, Voorhees JJ, Fisher GJ. Dermal damage promoted by repeated low-level UV-A1 exposure despite tanning response in human skin. JAMA Dermatol 2014;150:401–6.

Winkler B, Hoeffken HW, Eichin K, Houy W. A cyclic merocyanine UV-A absorber: mechanism of formation and crystal structure. Tetrahedron Lett 2014;55:1749–51.

York NR, Jacobe HT. UVA1 phototherapy: a review of mechanism and therapeutic application. Int J Dermatol 2010;49:623–30.

Yu SH, Bordeaux JS, Baron ED. The immune system and skin cancer. Adv Exp Med Biol 2014;810:182–91.